the FEBS Journal

Impact of the native-state stability of human lysozyme variants on protein secretion by *Pichia pastoris*

Janet R. Kumita[1], Russell J. K. Johnson[1], Marcos J. C. Alcocer[2], Mireille Dumoulin[1], Fredrik Holmqvist[3], Margaret G. McCammon[1], Carol V. Robinson[1], David B. Archer[3] and Christopher M. Dobson[1]

1 Department of Chemistry, University of Cambridge, UK
2 School of Biosciences, University of Nottingham, Loughborough, UK
3 School of Biology, University of Nottingham, UK

Keywords
amyloidosis; lysozyme; protein degradation; protein folding; protein secretion

Correspondence
C. M. Dobson, Department of Chemistry, Lensfield Road, University of Cambridge, Cambridge CB2 1EW, UK
Fax: +44 1223 763418
Tel: +44 1223 763070
E-mail: cmd44@cam.ac.uk

(Received 4 November 2005, revised 9 December 2005, accepted 12 December 2005)

doi:10.1111/j.1742-4658.2005.05099.x

We report the secreted expression by *Pichia pastoris* of two human lysozyme variants F57I and W64R, associated with systemic amyloid disease, and describe their characterization by biophysical methods. Both variants have a substantially decreased thermostability compared with wild-type human lysozyme, a finding that suggests an explanation for their increased propensity to form fibrillar aggregates and generate disease. The secreted yields of the F57I and W64R variants from *P. pastoris* are 200- and 30-fold lower, respectively, than that of wild-type human lysozyme. More comprehensive analysis of the secretion levels of 10 lysozyme variants shows that the low yields of these secreted proteins, under controlled conditions, can be directly correlated with a reduction in the thermostability of their native states. Analysis of mRNA levels in this selection of variants suggests that the lower levels of secretion are due to post-transcriptional processes, and that the reduction in secreted protein is a result of degradation of partially folded or misfolded protein via the yeast quality control system. Importantly, our results show that the human disease-associated mutations do not have levels of expression that are out of line with destabilizing mutations at other sites. These findings indicate that a complex interplay between reduced native-state stability, lower secretion levels, and protein aggregation propensity influences the types of mutation that give rise to familial forms of amyloid disease.

Human lysozyme is a well-characterized glycosidase that was first identified in 1922 by Alexander Fleming and normally functions as an antibacterial agent [1]. Since its discovery, the structure, folding and mechanism of action of the *c*-type lysozymes, which include the human form, have been studied extensively using a wide variety of techniques [2–14]. In the early 1990s, Pepys and co-workers reported that mutational variants of human lysozyme are associated with a hereditary non-neuropathic systemic amyloidosis [15]. This rare autosomal-dominant disease involves fibrillar deposits found to accumulate in a wide range of tissues including the liver, spleen and kidneys [15,16]. When samples of the *ex vivo* amyloid deposits from patients carrying the I56T or D67H mutation were analysed, the fibrils were found to contain only the full-length variants of lysozyme [15,17]. More recently, the occurrence of another natural variant of lysozyme with the T70N mutation has been reported [18,19]. The T70N mutation does not appear to cause amyloidosis, but

Abbreviations
ANS, 8-anilino-1-naphthalene sulfonic acid; BMG, buffered glycerol medium; BMM, buffered methanol medium; BPTI, bovine pancreatic trypsin inhibitor; PMSF, phenylmethanesulfonyl flouride; RD, regeneration dextrose; UV-vis, ultraviolet–visible; WT, wild-type; YNB, yeast nitrogen base; YPD, yeast peptone dextrose.

has an allele frequency of 5% in the British population, and has been identified in 12% of the white Canadian population [18,19].

Recombinant I56T, D67H and T70N lysozymes have been successfully expressed in a number of systems including baculovirus, *Saccharomyces cerevisiae*, *Pichia pastoris* and *Aspergillus niger*, enabling detailed studies of their folding and aggregation properties to be investigated [8,9,13,17,20,21]. The wild-type (WT) protein, in its native state, consists of an α- and a β-domain with four disulfide bonds (Fig. 1) [2,22]. All three variants have been found to have native-state structures that are similar to WT lysozyme and all possess enzymatic activity [8,17,20,21]. *In vitro* studies of the I56T and D67H variants have suggested that amyloid formation arises from a reduction in native-state stability and co-operativity relative to the WT protein [12,13,15,17,23]. An effectively identical, partially unfolded species which closely resembles the dominant intermediate populated during the refolding of the WT protein, has been found to be transiently populated under physiologically relevant conditions for both the I56T and D67H lysozyme [4,13,23]. In this intermediate, the region of the protein in the native state that forms the β-domain and the adjacent C-helix is simultaneously unfolded, whereas the regions that form helices A, B and D in the remainder of the α-domain maintain native-like structure. On this evidence it has been suggested that this transient, locally co-operative unfolding process is a crucial step in the events that lead to aggregation and amyloid fibril formation [12,13,23]. In the case of T70N, although the stability of the native state is lower than that of the WT protein, the transient and partially unfolded intermediate is not detectable *in vitro* under physiologically relevant conditions; however, it can be detected in both the T70N lysozyme and the WT protein under more destabilizing conditions [21].

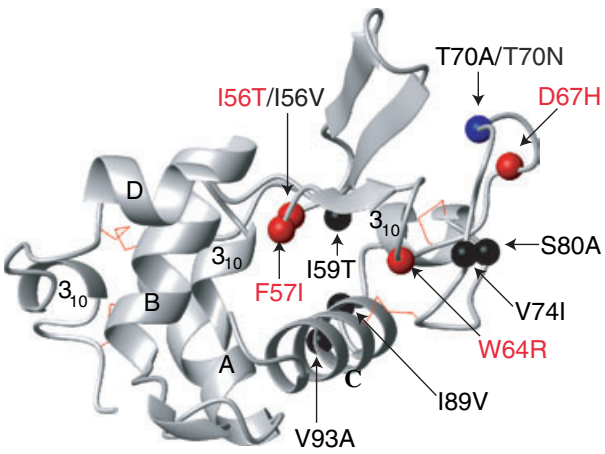

Fig. 1. Structure of human wild-type lysozyme and location of the mutations discussed in this study. The locations of the single-point mutations are shown on the structure of human wild-type lysozyme, defined by X-ray diffraction (PDB entry 1JSF). Known amyloidogenic mutations are shown in red, and the nonamyloidogenic, naturally occurring T70N mutant is shown in blue. All other mutations, which are not known to be naturally occurring, are shown in black α-helices in the α-domain are labelled A–D, along with 3_{10} helices. The four disulfide bridges are shown as red lines. The structure was produced by using MOLMOL [48].

Within the last five years, two novel variants of human lysozyme, F57I and W64R, have been identified by the detection of heterozygous, single-base mutations in the lysozyme gene of patients suffering from hereditary renal amyloidosis [19,24]. Amyloid deposits in patients carrying the W64R mutation were positively identified by a polyclonal lysozyme antibody; although the protein itself was not detected in the urine or plasma of these patients [24]. In the case of the F57I variant, amyloid deposits were present in patients possessing the F57I genetic mutation and in one case a second heterozygotic mutation was identified showing the presence of both the F57I and T70N mutations [19]. The discovery of two more naturally occurring lysozyme variants connected to amyloidosis is of major importance in the general context of the amyloid diseases, as it provides further information from which to develop a detailed understanding of why particular mutations lead to disease. More specifically, *in vitro* studies of these new variants will undoubtedly enhance our understanding of the common structural and biophysical attributes of variant lysozymes associated with disease.

We report here expression of the F57I and W64R lysozyme variants in *P. pastoris*. These two naturally occurring lysozyme variants display native-state thermostabilities that are reduced to a similar degree as that of the well-characterized I56T and D67H amyloidogenic variants, relative to WT protein. The secreted expression levels of all four amyloidogenic variants in *P. pastoris* are substantially compromised relative to WT lysozyme. To understand the factors that may contribute to this decrease in secreted yield, we investigated the secretion levels of a range of additional non-natural lysozyme variants that have previously been shown to maintain native overall structures, but to have varying native thermostabilities [10,25–29]. From this study, we demonstrate a clear relationship between the levels of protein secreted from *P. pastoris* and the native-state thermostability of the lysozyme variants, a finding that has implications for the onset and severity of amyloid disease in human patients.

Results

Secreted expression of the recently discovered F57I and W64R lysozyme variants from *P. pastoris* resulted in yields of 0.04 and 0.3 $mg{\cdot}L^{-1}$, respectively, based on UV–visible (UV-vis) spectroscopy; under similar expression conditions, WT lysozyme yielded 8.3 $mg{\cdot}L^{-1}$. The yields of the F57I and W64R variants were therefore lower, by factors of 200 and 30, respectively, relative to that of WT human lysozyme in these experiments. Under the same conditions, the I56T and D67H variants, both of which have been studied in detail previously were also secreted at low levels ($\approx$0.3 $mg{\cdot}mL^{-1}$), some 30 times less than that of WT lysozyme. To investigate the reason for these low expression levels, the secretion of a number of lysozyme variants that had been described previously [10,25–29], including the naturally occurring ones, I56T and T70N, was studied in more detail. As with the naturally occurring variants, the additional variants studied here have single amino acid substitutions in the β-domain or near the α/β-domain interface as shown in Fig. 1. The thermal denaturation behaviour of these mutants was monitored by far-UV CD (T_m) and by 8-anilino-1-naphthalene sulfonic acid (ANS) fluorescence emission ($T_{m\ ANS}$) and is shown in Table 1. A small-scale expression assay was utilized to compare quantitatively the levels of secreted protein for each lysozyme variant. Standard curve for enzymatic activity determined at 25 °C for each variant from purified protein samples, to account for differences in activity resulting from the various mutations (Table 2); the levels of activity were found to range from 65 to 100%. Lysozyme activity in the supernatant of each culture was therefore determined at 25 °C and compared with individual standard curves for the various proteins to determine the secreted yields. The yield ($mg{\cdot}L^{-1}$) was then divided by the OD_{600} of the culture and normalized to the WT control, allowing a comparison to be made between the levels of expression in the different experiments (Table 2). The results show a clear relationship between the thermal stability of each variant and the level of protein secreted to the supernatant (Fig. 2A), such that small changes in the T_m value can result in significant changes in secretion levels. To ensure that the lower levels of secretion were not due to intracellular protein accumulation, western blotting analysis was performed on cell lysates after various times of induction for two proteins (WT and W64R) and in both cases, no lysozyme was detected (data not shown).

To ensure that this correlation reflects post-transcriptional effects, and most likely changes in protein secretion, the mRNA levels of each lysozyme variant relative to the endogenous genetic reference β-actin, were determined by reverse transcriptase PCR analysis [30]. Comparison of the lysozyme-to-actin mRNA ratios for all the variants studied is shown in Fig. 2B. In all cases, the ratio lies in the range of 0.9–1.2, indicating that there are no appreciable differences in mRNA level for the different variants. This suggests that the origin of the decreased levels of secretion for

Table 1. Native-state thermostability of lysozyme variants.

Lysozyme variants	T_m (far-UV CD)	$T_{m\ ANS}$ (ANS fluorescence) pH 5.0[a]	$T_{m\ ANS}$ (ANS fluorescence) pH 6.0[b]
I56T	67.6 ± 0.8	65.3 ± 0.9	63.9 ± 1.7
I56V	75.8 ± 0.7	75.8 ± 0.7	–
F57I	–	–	60.4 ± 1.1
I59T	71.2 ± 0.4	70.1 ± 1.3	–
W64R	–	–	61.7 ± 1.0
D67H[c]	68.0 ± 1.0	66.0 ± 2.0	–
T70A	73.0 ± 0.7	73.1 ± 1.2	–
T70N	74.0 ± 0.6	74.8 ± 1.0	72.2 ± 0.9
V74I	78.3 ± 0.7	81.1 ± 2.0	–
S80A	77.9 ± 0.6	80.4 ± 1.9	–
I89V	75.9 ± 0.4	76.8 ± 1.0	–
V93A	76.1 ± 0.4	77.3 ± 1.2	–
WT	77.7 ± 0.5	79.2 ± 1.4	79.8 ± 1.2

[a] Analysis was performed on 2.0 μM protein, 0.1 M sodium citrate (pH 5.0) and 360 μM ANS. [b] Analysis was performed on 1.5 μM protein, 50 mM potassium phosphate (pH 6.0), 0.5 M NaCl, 360 μM ANS. These conditions were used to help alleviate aggregation of the F57I and W64R variants. [c] Previously reported values [13].

Table 2. Secreted protein levels of lysozyme variants expressed in *P. pastoris*.

Lysozyme variants	Yield ($mg{\cdot}L^{-1}$) per OD_{600} of 1.0[a]	Yield ($mg{\cdot}L^{-1}$) large-scale expression[b]	Per cent activity[c]
I56T	0.02 ± 0.01	0.3 ± 0.1	100[d]
I56V	0.65 ± 0.09	7.7 ± 1.0	100
F57I	–	0.04 ± 0.03	–
I59T	0.09 ± 0.04	1.1 ± 0.4	64
W64R	–	0.3 ± 0.1	–
T70A	0.12 ± 0.04	1.4 ± 0.8	70
T70N	0.20 ± 0.06	3.0 ± 0.8	70
V74I	1.11 ± 0.18	12.0 ± 2.0	95
S80A	1.06 ± 0.15	10.0 ± 2.0	85
I89V	0.81 ± 0.14	8.2 ± 1.0	85
V93A	0.57 ± 0.17	8.1 ± 0.8	95
WT	1.0	8.3 ± 1.1	100

[a] Values reported are the yield per OD_{600} of 1.0 for each variant relative to the yield of WT per OD_{600} of 1.0. [b] Performed in shaker flasks (in duplicate). [c] Per cent error of 10–25% based on three individual experiments for a protein concentration range of 0.2–0.9 $mg{\cdot}L^{-1}$ at 25 °C, pH 7.0. [d] Previously reported activity [17].

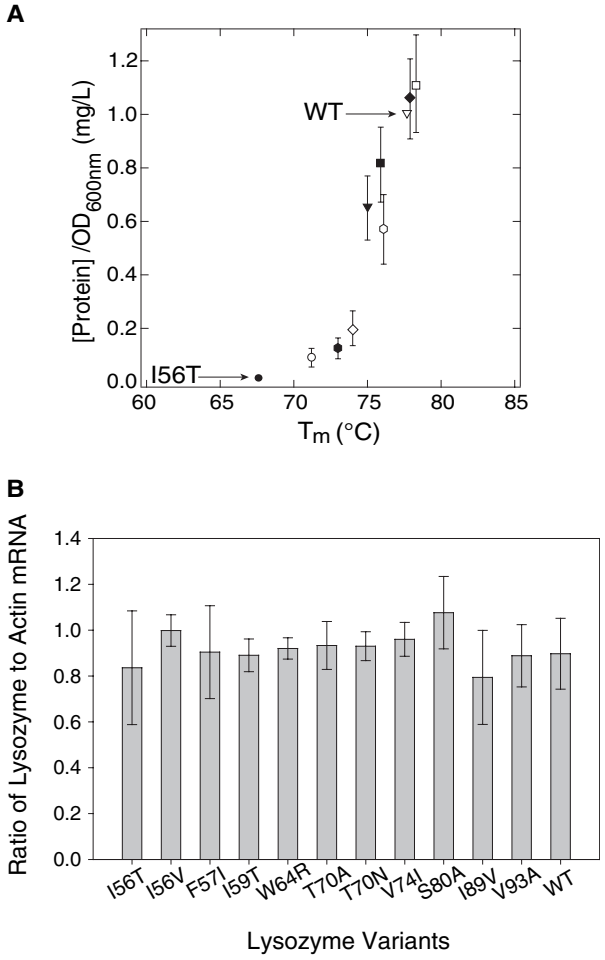

Fig. 2. Comparison of protein secretion levels and native-state stability. (A) Native-state stability, as measured by the mid-point temperature of unfolding (T_m) of each lysozyme variant (including WT protein), was plotted against the secretion level of each variant in *P. pastoris* (concentration/OD_{600}) (see Table 1 for values). The variants are I56T (●), I59T (○), T70A (⬢), T70N (◇), I56V (▼), I89V (■), V93A (◯), WT (▽), S80A (◆) and V74I (□). Values of protein expression are relative to cell density for each sample and have been normalized with respect to WT lysozyme (where WT expression/OD_{600} = 1.0). All points represent an average of 5–10 individual experiments. (B) Comparison of the relative mRNA levels for the lysozyme variants. RT-PCR was performed for the *P. pastoris* transformants of all the lysozyme variants. PCR levels of cDNA for each variant and its corresponding endogenous β-actin gene were analysed. The densities of the PCR products were determined, enabling the ratios of lysozyme to actin mRNA to be calculated. Comparison of the relative levels of mRNA indicates that no significant differences exist between the various transformants.

the less stable proteins is a result of degradation of partially folded or misfolded proteins by the quality control system during secretion. In light of the correlation between secreted protein levels and native-state thermostability, the lower secretion level of the amyloidogenic variant I56T can be seen to be consistent with its lower native-state stability and this suggests that the recently identified F57I and W64R variants may also be destabilized to a similar extent.

Of particular interest from the point of view of amyloid disease is the characterization of the two new mutational variants associated with clinical disease. Analysis of both the F57I and W64R variants, detected by SDS/PAGE analysis after ion-exchange purification, revealed a band at ≈14 kDa. ESI-MS analysis of the products showed that the samples all contain proteins with the masses anticipated for each variant (Fig. 3). Lysozyme activity, identified by the lysis of *Micrococcus lysodeikticus* cells, was detectable for both variants suggesting that the overall structure of the folded proteins is unlikely to differ significantly from that of the WT protein. The formation of a significant amount of one or more partially unfolded intermediates upon thermal unfolding has been well established for both the I56T and D67H amyloidogenic variants of lysozyme by monitoring changes in ANS fluorescence with increased temperature [13,17]. The origin of such changes is the presence of solvent-exposed hydrophobic clusters or surfaces resulting in a considerable increase in ANS fluorescence emission intensity, which is normally quenched in aqueous environments [31]. Moreover, in these two variants, the maximal ANS fluorescence intensity has been found to correspond closely with the midpoint of thermal denaturation (T_m) as determined by far-UV CD [13,17]. In accordance with these findings, for each of the variants analysed in this study the temperature of maximal ANS emission ($T_{m\,ANS}$) corresponds, within the bounds of experimental error, to the T_m determined by CD analysis at pH 5.0 (Table 1). Because of the low protein concentrations of F57I and W64R, measurement of the ANS fluorescence emission intensity was used to detect the presence of partially unfolded intermediates as well as to determine the thermostabilities of the native states of these variants (Fig. 4).

As the F57I and W64R variants had a marked tendency to aggregate, conditions were explored in order to overcome this problem, and the presence of 0.5 M NaCl was found to be optimal in helping to reduce the rate of aggregation. Using samples containing NaCl enabled reproducible spectroscopic analysis to be performed on samples immediately after purification (pH 6.0, 0.5 M NaCl) without the need for a dialysis step. For both these variants, significant ANS fluorescence was observed indicating that, like I56T and D67H, both variants populate partially unfolded species with increased exposure of their hydrophobic regions relative to WT protein (Fig. 4). The $T_{m\,ANS}$

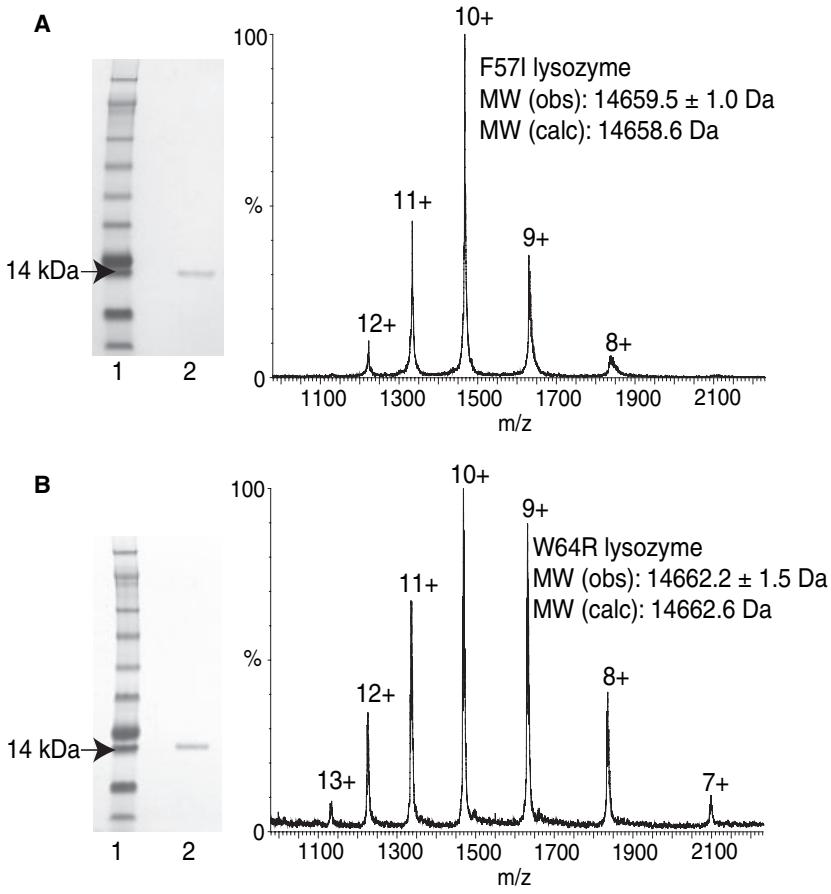

Fig. 3. Characterization of F57I and W64R lysozyme variants. The expression of the correct, full-length mutational variants was confirmed by SDS/PAGE (lane 1, standard protein markers; lane 2, lysozyme samples) and ESI-MS analyses for (A) F57I and (B) W64R. The ESI-MS samples were ≈10 μM in 1 : 1 water/acetonitrile with 2% acetic acid.

values for F57I and W64R, are 60.4 ± 1.1 and 61.7 ± 1.0 °C, respectively, and compare well with that of I56T under identical conditions (63.9 ± 1.7 °C) (Table 1); by contrast, the $T_{m\ ANS}$ of WT lysozyme is 79.8 ± 1.2 °C, a value which is in agreement with previous measurements. As with the previously studied amyloidogenic variants, I56T and D67H, the F57I and W64R variants clearly populate partially folded intermediates upon thermal denaturation, and the values of the midpoints of thermal denaturation are significantly lower than for the WT protein.

Discussion

The methylotropic yeast, *P. pastoris*, is an attractive expression system for our purposes because of the ease of its genetic manipulation [32] and the possibilities of using it to investigate the *in vivo* trafficking of amyloidogenic lysozyme variants in a manner similar to that described recently for α-synuclein by Outeiro & Lindquist [33]. In this study, we found that the secreted levels in *P. pastoris* of F57I and W64R, as well as of the I56T and D67H variants, are greatly reduced by comparison with that of the WT lysozyme. The initial spectroscopic investigations show that both F57I and W64R are destabilized to a remarkably similar degree to each other as well as to the well-characterized variants, I56T and D67H, i.e. with $T_{m\ ANS}$ values lower by ≈18 ± 2 °C than that of the WT protein. Moreover, examination of the location of the naturally occurring mutations in the native structure of lysozyme shows that the I56T and F57I mutations lie at the interface between the α- and β-domains. In addition, the D67H mutation, although located in the long loop of the β-domain (where W64R is also located), disrupts a series of hydrogen bonds resulting in significant structural perturbations in the vicinity of the α/β interface [17]. The T70N mutation also lies in the long loop of the β-domain and structural analysis shows that the native structure of this variant is perturbed so as to lie intermediate between the D67H variant and WT protein [21]; however, T70N does not result in as significant a reduction in native stability as the other variants (only ≈4 °C less stable than WT) [21], and interestingly, has not been found in amyloidogenic deposits [19,20]. Our results for F57I and W64R

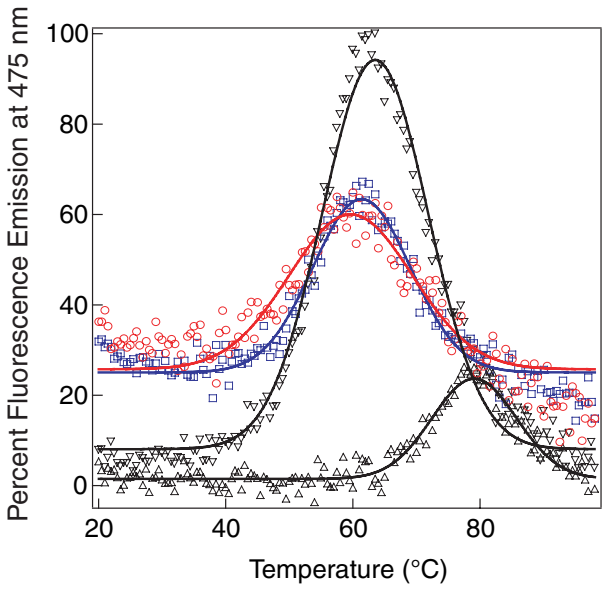

Fig. 4. Thermal denaturation of F57I and W64R variants in the presence of ANS. ANS fluorescence emission during thermal denaturation of I56T (▽), WT (△), F57I (○) and W64R (□). Solid lines indicate fitted curves. All samples were performed in duplicate with 1.5 μM protein, 50 mM potassium phosphate buffer (pH 6.0), 0.5 M NaCl, and 360 μM ANS.

strongly support the idea that the disruption of the interface region is of great importance in the process which leads to fibril formation [12,13,23]. In addition to these findings, by systematically investigating the secreted levels of a larger number of lysozyme variants, a highly significant correlation has been identified between the level of secreted protein and the thermostability of the native state of the protein (Fig. 2A). This correlation shows that even small changes in the protein native stability can have a dramatic effect on the amount of secreted protein in the medium. Also, the relationship between native-state thermostability and secretion levels, shown in the set of variants analysed in this study, can by itself account for the relatively low expression levels of the amyloidogenic variants in this system. Importantly, our result shows that human disease-associated mutations in this study do not have levels of expression that are out of line with destabilizing mutations at other sites. Positive correlations between thermostability and protein expression have also been found in *S. cerevisiae* for mutants of bovine pancreatic trypsin inhibitor (BPTI) [34], insulin [35], hen egg white lysozyme [36], and single-chain T-cell receptor [37]. It has been previously shown that a maximal plateau in expression level is reached as the thermostability increases for mutants of BPTI [34]. If this were to hold true for human lysozyme, a sigmoidal relationship between thermal stability and secretion would be observed, although experimental confirmation of this prediction will require the discovery of variants with higher native stabilities than even the V74I and S80A lysozymes (see Fig. 2A).

Despite the clear correlation observed here between native-state thermostability and secretion levels in *P. pastoris* and *S. cerevisiae*, reports in the literature suggest that there could be exceptions to such a relationship. The EAEA-lysozyme and C77/95A variants of human lysozyme, for example, have been shown to be thermally destabilized with respect to WT protein, although, this does not appear to have a detrimental effect on protein expression in yeast [38,39]. Investigations of the effect of thermostability on protein secretion and aggregation have also been performed in other organisms including *Escherichia coli*, and in mammalian cells [40–42]. In some instances, a relationship between native-state stability and aggregation has been seen [40], whereas in others, straightforward correlations were not observed and other factors were found to contribute to a relationship [41,42]. Interestingly, in the EAEA-lysozyme and C77/95A variants, the modifications are not just single-point mutations, but include the incorporation of additional residues at the N-terminus and the removal of a disulfide bond. These findings suggest that the nature and location of the destabilizing mutations and factors such as the presence or absence of disulfide bonds may play an important role in the secretion efficiency. Moreover, from this study it is evident that the native states of all four of the mutational variants of human lysozyme that are known to be linked with disease are destabilized to a remarkably similar extent, and all have dramatically decreased secretion efficiency in *P. pastoris*. In light of this finding it appears that circumstances in which the balance between secretion levels, native-state stability and aggregation tendencies combine to result in significant levels of aggregation *in vivo* could be relatively limited. Such a conclusion would explain why familial forms of amyloid disease are relatively rare, despite the fact that *in vitro* many proteins are able to convert into the types of aggregate associated with pathogenic behaviour.

Experimental procedures

All restriction enzymes were purchased from New England Biolabs Ltd. (Hitchin, UK). PfuTurbo DNA polymerase was purchased from Stratagene Europe (Amsterdam, the Netherlands). Synthetic oligonucleotides were purchased from Operon (Cologne, Germany). All chemicals were purchased from Sigma-Aldrich (Gillingham, UK) unless otherwise stated.

Plasmids and strains

E. coli DH5α cells (Invitrogen, Paisley, UK) were used for the propagation of plasmids and *P. pastoris* GS115 (Invitrogen) was used as a host strain for lysozyme expression. A pPIC9-based plasmid containing the cDNA sequence encoding mature WT human lysozyme was constructed according to the supplier's instructions (Invitrogen). In order to direct the expressed protein into the secretory pathway, the cDNA sequence was fused with the methanol-inducible 5′-AOX1 promoter, the sequence encoding the α-factor secretion signal [43,44], and the 3′-AOX transcriptional terminator. The amino acids that constitute the Kex2 processing site were included in the sequence to facilitate proteolytic processing during secretion. Site-directed mutagenesis was performed on pPIC9 containing the WT human lysozyme gene using the QuikChange Site-Directed Mutagenesis protocol (Stratagene Europe). All mutations were confirmed by DNA sequencing, performed at the Sequencing Facility in the Department of Biochemistry at Cambridge University.

Transformation of *P. pastoris*

The pPIC9 plasmid containing the lysozyme gene was linearized by *Stu*I digestion followed by butanol precipitation. Transformation of *P. pastoris* was performed with a Bio-Rad MicroPulser electroporation apparatus, following the manufacturer's instructions (Bio-Rad, Hemel Hempsted, UK). The transformed cells were grown on RD media plates [1 M sorbitol, 2% dextrose, 1.34% yeast nitrogen base (YNB), 4.0×10^{-5}% biotin] for 48–72 h at 30 °C. Ninety-six colonies of each variant were screened for lysozyme activity. Single colonies were used to inoculate 1 mL YPD medium (1% yeast extract, 2% peptone, 2% dextrose) in 24-well plates. The cells were incubated at 30 °C for 18 h, 1 mL YPD was added and the incubation was continued for 48 h. The plates were then centrifuged (3500 ***g***, 10 min, 4 °C) and the supernatant removed. The cells were resuspended in buffered methanol medium (BMM; 100 mM potassium phosphate pH 6.0, 1.34% YNB, 4.0×10^{-5}% biotin, 0.5% methanol) to induce lysozyme expression. Methanol (0.5% v/v) was replenished every 12 h until expression was terminated at 72 h. The plates were centrifuged (3500 ***g***, 10 min, 4 °C) and the supernatant was analysed for lysozyme activity by monitoring the lysis of the cell walls of *M. lysodeikticus* (Sigma-Aldrich) in 96-well microplates [45]. For each variant, colonies which displayed the greatest lysozyme activity in the supernatant were used for larger scale expression.

Secreted expression of lysozyme variants

Pre-cultures (6 mL) were started in buffered glycerol medium (BMG; 100 mM potassium phosphate pH 6.0, 1.34% YNB, 4×10^{-5}% biotin, 1% glycerol) for each lysozyme variant. These cultures were incubated for 36 h (30 °C, 230 r.p.m.), and a 1 : 100 dilution was made into 400 mL BMG and incubated for 24 h (30 °C, 230 r.p.m.). The BMG cultures (200 mL) were centrifuged (5000 ***g***, 4 °C, 10 min) and the supernatants discarded. The yeast pellets were resuspended in BMM to induce protein expression and induction was performed for 72 h (30 °C, 230 r.p.m.) with 0.5% methanol being replenished every 12–24 h. After induction, the cultures were centrifuged (9000 ***g***, 4 °C, 10 min), and the pellets discarded. The supernatant was then centrifuged a second time (9000 ***g***, 4 °C, 10 min) and filtered. Purification of lysozyme from the supernatant was performed on a HS20 cation-exchange POROS column (Applied Biosystems, Warrington, UK) on a BioCAD 700E system (Applied Biosystems). Lysozyme was eluted at ≈55 mS by a linear NaCl gradient. The protein peaks were analysed by SDS/PAGE and the relevant fractions were dialysed against water for between 48 and 72 h and then lyophilized. The purity of the proteins was confirmed by SDS/PAGE and molecular masses were determined by ESI-MS. Spectra were acquired over a range of 500–5000 Da on an LCT MS (Waters Ltd, Elstree, UK) equipped with a nanoflow Z-spray source and calibrated using CsI (15 μM). Data were analysed using MASSLYNX 3.4 (Waters Ltd) with molecular masses calculated from the centroid values of at least three charge states. All mass spectra are presented as raw data with minimal smoothing and without resolution enhancement.

Small-scale expression assay for lysozyme variants

To compensate for fluctuations in day-to-day conditions, small-scale expression of all the variants was performed in parallel, using WT lysozyme as a control sample. BMG (5 mL) was inoculated from glycerol stocks of each variant and incubated for 48 h (30 °C, 230 r.p.m). The samples were then centrifuged (5000 ***g***, 4 °C, 15 min) and the supernatant discarded. The pellets were resuspended in BMM (10 mL) and protein expression was induced for 72 h with 0.5% methanol being replenished every 24 h. After 72 h, the OD_{600} of a 1 : 10 cell culture was determined for each sample. The samples were centrifuged (5000 ***g***, 4 °C, 15 min) and in each case, the supernatant was analysed for lysozyme activity. Because the specific activity of the native protein differed for each variant (ranging from 65 to 100% of WT), the quantity of lysozyme produced was determined in each case by comparing the rate of lysis to standard curves (0.2–0.9 $mg \cdot L^{-1}$) determined for each purified variant (25 °C, pH 7.0). Protein concentrations are reported as values which take into consideration the differences in cell culture growth (OD_{600}), and these values were further normalized with respect to the WT lysozyme control within each data set to allow comparison without day-to-day variations.

SDS/PAGE and western blotting

Cell pellets from the small scale expression (before and after induction at time points between 5 and 96 h) for WT and W64R lysozyme variants were suspended in 50 mM sodium phosphate buffer (pH 7.4) containing 1 mM EDTA, 5% glycerol and 1 mM phenylmethylsulfonyl fluoride (PMSF) (added fresh daily). The cells were lysed by vortexing the samples in the presence of acid-washed glass beads (425–600 microns) (Sigma-Aldrich). SDS/PAGE analysis of these samples, as well as the supernatants (after induction) of the WT and W64R lysozyme variants and purified WT lysozyme (control sample) was performed on 4–12% Bis-Tris NuPAGE gels (Invitrogen) in Mes buffer under reducing conditions. Transfer of the proteins from the SDS/PAGE gel onto polyvinylidene difluoride membrane (0.45 μm pore size) was performed in Tris-glycine buffer containing 20% methanol and 0.01% SDS, using an XCell II Blot module (Invitrogen) with a constant voltage (30 V, 1.5 h). The blot was probed with an antilysozyme monoclonal camelid serum fragment (cAb-HuL6) containing a His-tag [12] and detected with an anti-His (C-terminal) serum conjugated to alkaline phosphatase (Invitrogen). The blot was developed using a Westernbreeze^{TM} Immunodetection kit (Invitrogen). Lysozyme was present in the control sample and the WT supernatant; however, no evidence for lysozyme was present for the cell lysates of both WT and W64R lysozymes after both 5 and 96 h of induction. The same cell lysate samples were analysed by the enzymatic activity assay detailed by Lee and co-workers [45]. Activity was detected in the supernatant and cell lysate samples for the WT variant at different time points, although the activity observed in the WT cell lysate samples was very low ($< 10\%$ of the activity that was observed in the supernatant). No activity was observed in the supernatant or cell lysate samples of the W64R variant.

Comparison of mRNA levels

The total RNA content of the *P. pastoris* strains containing each lysozyme variant gene was isolated using a Qiagen RNeasy Mini prep kit (Qiagen, Cologne, Germany), and 2 μg quantities were treated with DNase (Promega, Southampton, UK) following the manufacturer's protocol. The DNase-treated total RNA was separated into two equal aliquots (1 μg total RNA). One aliquot was used for cDNA synthesis of lysozyme and the other one for cDNA synthesis of actin using Improm II reverse transcriptase (Promega). PCR analysis of the cDNA samples was performed using T7 Pfu turbo polymerase. The levels of DNA production over the course of PCR analysis were monitored to determine the linear region of amplification. Once determined, lysozyme and actin cDNA amplification was analysed in parallel (cycles 22–26). The samples were separated on 2% E-gels (Invitrogen), and the densities of the lysozyme and actin bands were determined using Scion Image (Scion Corp, Frederick, MD). The ratio of the density of lysozyme to actin was determined for each variant for direct comparison of their mRNA levels. All experiments were performed in triplicate.

Thermal denaturation followed by CD and fluorescence

Protein concentrations were determined by UV-spectroscopy as described previously [17]; for W64R, an estimated extinction coefficient of 30 920 $M^{-1}cm^{-1}$ was used, based on its amino acid composition [46]. Thermal denaturation studies were performed at pH 5.0 for direct comparison with previous studies. For F57I and W64R, ANS denaturation studies were performed at pH 6.0 in the presence of NaCl to alleviate problems with protein solubility. Thermal denaturation of the variants was monitored by far-UV CD at 222 nm in a Jasco J-810 spectropolarimeter (JASCO Ltd, Great Dunmow, UK). Samples were analysed using a 0.1 cm path-length cell with a protein concentration of 13.6 μM in 10 mM sodium citrate (pH 5.0). The temperature was increased from 20 to 95 °C at a rate of 0.5 °C·min^{-1}. All experiments were performed in triplicate unless otherwise stated. Ellipticity values were normalized to the fraction of unfolded protein (F_u) using $F_u = (\theta - \theta_N)/(\theta_U - \theta_N)$ where θ = observed ellipticity, θ_N = native ellipticity and θ_U = unfolded ellipticity. θ_N and θ_U were extrapolated from pre- and post-transition baselines at the relative temperature. Experimental data were fitted with a sigmoidal expression [47], using KALEIDAGRAPH (Synergy Software, Reading, MA). T_m is defined as the temperature where the fraction of unfolded protein is 0.5. Thermal denaturation monitored by ANS fluorescence emission was recorded on a Cary Eclipse spectrofluorimeter (Varian Ltd, Oxford, UK) using excitation and emission wavelengths of 350 and 475 nm, respectively, with slit widths of 5 nm. The temperature was increased from 20 to 95 °C at a rate of 0.5 °C·min^{-1}. Unless stated, analysis was performed on 2.0 μM protein in 0.1 M sodium citrate (pH 5.0) and containing 360 μM ANS. A control sample of ANS only (360 μM) was performed and this was subtracted from all samples to take into consideration the effects of temperature on ANS fluorescence. Fluorescence was normalized with respect to the I56T lysozyme emission spectrum. Experimental data were fitted with a Gaussian expression using SIGMAPLOT (Systat Software UK Ltd, London UK). $T_{m\ ANS}$ is defined as the temperature where the ANS fluorescence emission was at its maximum.

Acknowledgements

We would like to thank Gemma Caddy (University of Cambridge) for assistance with ESI-MS analysis, Alain

Brans and Fabrice Bouillenne at the University of Liège for assistance with protein expression and John Christodoulou for critical reading of the manuscript. JRK is supported by a Natural Sciences and Engineering Research Council of Canada (NSERC) Post-doctoral fellowship. RJKJ is supported by a BBSRC Studentship. The research of CMD is supported, in part, by Programme Grants from the Wellcome Trust and the Leverhulme Trust. This study has also been supported by a BBSRC grant (CMD, CVR, DBA).

References

1 Fleming A (1922) On a remarkable bacteriolytic element found in tissues and secretions. *Proc R Soc Lond B* **93**, 306–317.
2 Artymiuk PJ & Blake CCF (1981) Refinement of human lysozyme at 1.5 Å resolution analysis of non-bonded and hydrogen-bond interactions. *J Mol Biol* **152**, 737–762.
3 Taniyama Y, Yamamoto Y, Kuroki R & Kikuchi M (1990) Evidence for difference in the roles of two cysteine residues involved in disulfide bond formation in the folding of human lysozyme. *J Biol Chem* **265**, 7570–7575.
4 Hooke SD, Radford SE & Dobson CM (1994) The refolding of human lysozyme: a comparison with the structurally homologous hen lysozyme. *Biochemistry* **33**, 5867–5876.
5 Hooke SD, Eyles SJ, Miranker A, Radford SE, Robinson CV & Dobson CM (1995) Cooperative elements in protein folding monitored by electrospray ionization mass spectrometry. *J Am Chem Soc* **117**, 7548–7549.
6 Haezebrouck P, Joniau M, Van Dael H, Hooke SD, Woodruff ND & Dobson CM (1995) An equilibrium partially folded state of human lysozyme at low pH. *J Mol Biol* **246**, 382–387.
7 Muraki M & Harata K (1996) Origin of carbohydrate recognition specificity of human lysozyme revealed by affinity labeling. *Biochemistry* **35**, 13562–13567.
8 Funahashi J, Takano K, Ogasahara K, Yamagata Y & Yutani K (1996) The structure, stability, and folding process of amyloidogenic mutant human lysozyme. *J Biochem (Tokyo)* **120**, 1216–1223.
9 Canet D, Sunde M, Last AM, Miranker A, Spencer A, Robinson CV & Dobson CM (1999) Mechanistic studies of the folding of human lysozyme and the origin of amyloidogenic behavior in its disease-related variants. *Biochemistry* **38**, 6419–6427.
10 Funahashi J, Takano K, Yamagata Y & Yutani K (2000) Role of surface hydrophobic residues in the conformational stability of human lysozyme at three different positions. *Biochemistry* **39**, 14448–14456.
11 Takano K, Funahashi J & Yutani K (2001) The stability and folding process of amyloidogenic mutant human lysozymes. *Eur J Biochem* **268**, 155–159.
12 Dumoulin M, Last AM, Desmyter A, Decanniere K, Canet D, Larsson G, Spencer A, Archer DB, Sasse J, Muyldermans S *et al.* (2003) A camelid antibody fragment inhibits the formation of amyloid fibrils by human lysozyme. *Nature* **424**, 783–788.
13 Dumoulin M, Canet D, Last AM, Pardon E, Archer DB, Muyldermans S, Wyns L, Matagne A, Robinson CV, Redfield C *et al.* (2005) Reduced global cooperativity is a common feature underlying the amyloidogenicity of pathogenic lysozyme mutations. *J Mol Biol* **346**, 773–788.
14 Dumoulin M, Bellotti V & Dobson CM (2005) Hereditary systemic amyloidosis associated with mutational variants of human lysozyme. *Amyloid Proteins: The Beta Pleated Sheet Conformation and Disease* (Sipe J, ed.), pp. 635–656. Wiley-VCH-Verlag, Weinheim.
15 Pepys MB, Hawkins PN, Booth DR, Vigushin DM, Tennent GA, Soutar AK, Totty N, Nguyen O, Blake CCF, Terry CJ *et al.* (1993) Human lysozyme gene mutations cause hereditary systemic amyloidosis. *Nature* **362**, 553–557.
16 Gillmore JD, Booth DR, Madhoo S, Pepys MB & Hawkins PN (1999) Hereditary renal amyloidosis associated with variant lysozyme in a large English family. *Nephrol Dial Transplant* **14**, 2639–2644.
17 Booth DR, Sunde M, Bellotti V, Robinson CV, Hutchinson WL, Fraser PE, Hawkins PN, Dobson CM, Radford SE, Blake CCF *et al.* (1997) Instability, unfolding and aggregation of human lysozyme variants underlying amyloid fibrillogenesis. *Nature* **385**, 787–793.
18 Booth DR, Pepys MB & Hawkins PN (2000) A novel variant of human lysozyme (T70N) is common in the normal population. *Hum Mutat* **16**, 180.
19 Yazaki M, Farrell SA & Benson MD (2003) A novel lysozyme mutation Phe57Ile associated with hereditary renal amyloidosis. *Kidney Int* **63**, 1652–1657.
20 Esposito G, Garcia J, Mangione P, Giorgetti S, Corazza A, Viglino P, Chiti F, Andreola A, Dumy P, Booth D *et al.* (2003) Structural and folding dynamics properties of T70N variant of human lysozyme. *J Biol Chem* **278**, 25910–25918.
21 Johnson RJK, Christodoulou J, Dumoulin M, Caddy G, Alcocer MJ, Murtagh GJ, Kumita JR, Larsson G, Robinson CV, Archer DB *et al.* (2005) Rationalising lysozyme amyloidosis: insight from the structure and solution dynamics of T70N lysozyme. *J Mol Biol* **352**, 823–836.
22 Harata K, Abe Y & Muraki M (1998) Full-matrix least-squares refinement of lysozymes and analysis of anisotropic thermal motion. *Prot Struct Funct Genet* **30**, 232–243.
23 Canet D, Last AM, Tito P, Sunde M, Spencer A, Archer DB, Redfield C, Robinson CV & Dobson CM

(2002) Local cooperativity in the unfolding of an amyloidogenic variant of human lysozyme. *Nat Struct Biol* **9**, 308–315.
24 Valleix S, Drunat S, Philit JB, Adoue D, Piette JC, Droz D, MacGregor B, Canet D, Delpech M & Grateau G (2002) Hereditary renal amyloidosis caused by a new variant lysozyme W64R in a French family. *Kidney Int* **61**, 907–912.
25 Takano K, Ogasahara K, Kaneda D, Yamagata Y, Fujii S, Kanaya E, Kikuchi M, Oobatake M & Yutani K (1995) Contribution of hydrophobic residues to the stability of human lysozyme: caliometric studies and X-ray structural analysis of the five isoleucine to valine mutants. *J Mol Biol* **254**, 62–76.
26 Takano K, Yamagata Y, Fujii S & Yutani K (1997) Contribution of the hydrophobic effect to the stability of human lysozyme: calorimetric studies and X-ray structural analyses of the nine valine to alanine mutants. *Biochemistry* **36**, 688–698.
27 Takano K, Yamagata Y, Kubota M, Funahashi J, Fujii S & Yutani K (1999) Contribution of hydrogen bonds to the conformational stability of human lysozyme: calorimetry and X-ray analysis of six Ser to Ala mutants. *Biochemistry* **38**, 6623–6629.
28 Funahashi J, Takano K, Yamagata Y & Yutani K (1999) Contribution of amino acid substitutions at two different interior positions to the conformational stability of human lysozyme. *Protein Eng* **12**, 841–850.
29 Takano K, Yamagata Y, Funahashi J, Hioki Y, Kuramitsu S & Yutani K (1999) Contribution of intra- and intermolecular hydrogen bonds to the conformational stability of human lysozyme. *Biochemistry* **38**, 12698–12708.
30 Horikoshi T & Sakakibara M (2000) Quantification of relative mRNA expression in the rat brain using simple RT-PCR and ethidium bromide staining. *J Neurosci Methods* **99**, 45–51.
31 Engelhard M & Evans PA (1995) Kinetics of interaction of partially folded proteins with a hydrophobic dye: evidence that molten globule character is maximal in early folding intermediates. *Protein Sci* **4**, 1553–1562.
32 Cereghino GP, Cereghino JL, Ilgen C & Cregg JM (2002) Production of recombinant proteins in fermenter cultures of the yeast *Pichia pastoris*. *Curr Opin Biotechnol* **13**, 329–332.
33 Outeiro TF & Lindquist S (2003) Yeast cells provide insight into alpha-synuclein biology and pathobiology. *Science* **302**, 1772–1775.
34 Kowalski JM, Parekh RN & Wittrup KD (1998) Secretion efficiency in *Saccharomyces cerevisiae* of bovine pancreatic trypsin inhibitor mutants lacking disulfide bonds is correlated with thermodynamic stability. *Biochemistry* **37**, 1264–1273.
35 Kjeldsen T & Pettersson AF (2003) Relationship between self association of insulin and its secretion efficiency in yeast. *Protein Expr Purif* **27**, 331–337.
36 Song Y, Sakai J, Usui M, Azakami H & Kato A (2002) Relationship between the stability of lysozymes mutated at the inside hydrophobic core and secretion in *Saccharomyces cerevisisae*. *Nahrung* **46**, 209–213.
37 Shusta EV, Kieke MC, Parke E, Kranz DM & Wittrup KD (1999) Yeast polypeptide fusion surface display levels predict thermal stability and soluble secretion efficiency. *J Mol Biol* **292**, 949–956.
38 Goda S, Takano K, Yamagata Y, Katakura Y & Yutani K (2000) Effect of extra N-terminal residues on the stability and folding of human lysozyme expressed in *Pichia pastoris*. *Protein Eng* **13**, 299–307.
39 Taniyama Y, Ogasahara K, Yutani K & Kikuchi M (1992) Folding mechanism of mutant human lysozyme C77/95A with increased secretion efficiency in yeast. *J Biol Chem* **267**, 4619–4624.
40 Calloni G, Zoffoli S, Stefani M, Dobson CM & Chiti F (2005) Investigating the effects of mutations on protein aggregation in the cell. *J Biol Chem* **280**, 10607–10613.
41 Chrunyk BA, Evans J, Lillquist J, Young P & Wetzel R (1993) Inclusion body formation and protein stability in sequence variants of interleukin-1β. *J Biol Chem* **268**, 18053–18061.
42 Sekijima Y, Wiseman RL, Matteson J, Hammarström P, Miller SR, Sawkar AR, Balch WE & Kelly JW (2005) The biological and chemical basis for tissue selective amyloid disease. *Cell* **121**, 73–85.
43 Brake AJ, Merryweather JP, Coit DG, Heberlein UA, Masiarz FR, Mullenbach GT, Urdea MS, Valenzuela P & Barr PJ (1984) α-Factor-directed synthesis and secretion of mature foreign proteins in *Saccharomyces cerevisiae*. *Proc Natl Acad Sci USA* **81**, 4642–4646.
44 Oka C, Tanaka M, Muraki M, Harata K, Suzuki K & Jigami Y (1999) Human lysozyme secretion increased by alpha-factor pro-sequence in *Pichia pastoris*. *Biosci Biotechnol Biochem* **63**, 1977–1983.
45 Lee YC & Yang D (2002) Determination of lysozyme activities in a microplate format. *Anal Biochem* **310**, 223–224.
46 Gill SC & von Hippel PH (1989) Calculation of protein extinction coefficients from amino acid sequence data. *Anal Biochem* **182**, 319–326.
47 Mombelli E, Afshar M, Fusi P, Mariani M, Tortora P, Connelly JP & Lange R (1997) The role of phenylalanine 31 in maintaining the conformational stability of ribonuclease P2 from *Sulfolobus solfataricus* under extreme conditions of temperature and pressure. *Biochemistry* **36**, 8733–8742.
48 Koradi R, Billeter M & Wuthrich K (1996) MOLMOL: a program for display and analysis of macromolecular structures. *J Mol Graph* **14** (51–5), 29–32.